Cutaneous Exposure to Arsenicals Is Associated with Development of Constrictive Bronchiolitis in Mice

Ranu Surolia[1,2], Fu Jun Li[1,2], Kevin Dsouza[1,2], Huaxiu Zeng[1], Pooja Singh[1,2], Crystal Stephens[1,2], Yuanyuan Guo[3], Zheng Wang[1], Mahendra Kashyap[3], Ritesh Srivastava[3], Manuel Lora Gonzalez[4], Paul Benson[4], Abhishek Kumar*, Harrison Kim[5], Young-il Kim[1], Aftab Ahmad[6‡], Mohammad Athar[3‡], and Veena B. Antony[1,2‡]

[1]Division of Pulmonary, Allergy, and Critical Care Medicine, Department of Medicine, [3]Department of Dermatology, [4]Department of Pathology, [5]Department of Radiology, [6]Department of Anesthesiology and Perioperative Medicine, and [2]Superfund Research Center, University of Alabama at Birmingham, Birmingham, Alabama

ORCID IDs: 0000-0001-5389-3584 (R.S.); 0000-0003-0686-0987 (A.A.).

Abstract

Organoarsenicals, such as lewisite and related chloroarsine, diphenylchloroarsine (DPCA), are chemical warfare agents developed during World War I. Stockpiles in Eastern Europe remain a threat to humans. The well-documented effects of cutaneous exposure to these organoarsenicals include skin blisters, painful burns, and life-threatening conditions such as acute respiratory distress syndrome. In survivors, long-term effects such as the development of respiratory ailments are reported for the organoarsenical sulfur mustard; however, no long-term pulmonary effects are documented for lewisite and DPCA. No animal models exist to explore the relationship between skin exposure to vesicants and constrictive bronchiolitis. We developed and characterized a mouse model to study the long-term effects of cutaneous exposure on the lungs after exposure to a sublethal dose of organoarsenicals. We exposed mice to lewisite, DPCA, or a less toxic surrogate organoarsenic chemical, phenyl arsine oxide, on the skin. The surviving mice were followed for 20 weeks after skin exposure to arsenicals. Lung microcomputed tomography, lung function, and histology demonstrated increased airway resistance, increased thickness of the smooth muscle layer, increased collagen deposition in the subepithelium, and peribronchial lymphocyte infiltration in mice exposed to arsenical on skin.

Keywords: chemical warfare agents; delayed lung injury; constrictive bronchiolitis

Organoarsenicals lewisite and Clark I are chemical war-threat agents developed during World War I (WWI). Lewisite (dichloro [2-chlorovinyl] arsine), is a vesicant class chemical agent, whereas Clark I (diphenylchloarsine [DPCA]), commonly known as Clark I, is a chemical agent that induces retching and sneezing (sternutatory agent) with vesicant properties (1). The 1925 Geneva Protocol prohibits the use of chemical war agents in international armed conflicts; hence, the use of lewisite or any other chemicals is prohibited. Yet stockpiles and unmarked burial sites of lewisite still exist in different countries. There are rising

(Received in original form August 15, 2022; accepted in final form February 13, 2023)

*Copyeditor and Statistical Analyst; Member, UAB Superfund Advisory Board.

‡Co–senior authors.

Supported by the CounterACT Program, the National Institutes of Health Office of the Director, and National Institute of Environmental Health Sciences grants U54ES030246 (V.B.A. [project leader], A.A., and M.A. [PI]), R01 ES029981 (V.B.A.), and P42ES027723 (V.B.A.). The study sponsors had no involvement in the study design, collection, analysis and interpretation of data, the writing of the manuscript, or the decision to publish the manuscript.

Author Contributions: R. Surolia and V.B.A. conceived and designed the experiments, performed the experiments, analyzed the data, and wrote the manuscript. R. Surolia, F.L., K.D., H.Z., C.S., M.K., R. Srivastava, Z.W., and P.S. performed the experiments. H.K. performed and analyzed radiology experiments. R. Surolia, M.K., H.Z., R. Srivastava and Z.W. contributed with the animal exposure experiments. M.L.G. and P.B. performed pathological analysis of the histology of lungs. Y.K. performed biostatistical analyses. A.K. assisted in revising the manuscript. A.A., M.A., and V.B.A. conceived the project, designed the experiments, and revised the manuscript.

Correspondence and requests for reprints should be addressed to Veena B. Antony, M.D., Division of Pulmonary, Allergy, and Critical Care Medicine, Department of Medicine, University of Alabama at Birmingham and Superfund Research Center at UAB, 901 19th Street South, BMR2, Room 404, Birmingham, AL 35294. E-mail: vantony@uabmc.edu.

This article has a data supplement, which is accessible from this issue's table of contents at www.atsjournals.org.

Am J Respir Cell Mol Biol Vol 68, Iss 5, pp 485–497, May 2023

Originally Published in Press as DOI: 10.1165/rcmb.2022-0321MA on February 13, 2023
Internet address: www.atsjournals.org

concerns about the possible use of chemical threat agents in the ongoing Ukraine–Russia conflict. Accidental exposures at stockpile facilities, unknown burial sites, unexpected environmental release from stockpiles/burial sites, and unethical use in wars are major risk factors for the exposure to lewisite. The most recent use of lewisite was during the Iran–Iraq war (2–4). Accidental exposures to lewisite in humans are reported in Japanese gas factories during WWII (5, 6). Lewisite inflicts instant painful severe local blistering and burns, instant edema, blepharospasm and superficial opacities in eyes (7), and respiratory failure (6, 8, 9). DPCA causes nausea, vomiting, and headaches and also induces pulmonary edema (10).

Lewisite acts as a systemic poison, and the moist tissues such as the eyes and lungs are most vulnerable to toxic effects after primary skin exposure (8). Even though there is an absence of a cohesive body of literature to document the effects of acute exposure of lewisite on lungs, the clinical features of acute exposure-associated lung injury are well understood (8). An animal model study showed that DPCA burns are accompanied by acute systemic effects on lungs (11). There is not much known about the long-term effects of lewisite and DPCA exposure on lungs. The guidelines for treating chemical threat–related casualties are palliative because of limited records and understanding of specific mechanisms of toxicity (12, 13). WWI and postwar research programs used skin injuries and burns as endpoints of their research and had no follow-up on human subjects.

Few historical records and public hearing reports documented that lewisite and sulfur mustard (SM) instigated long-term effects in the lungs of the victims of gas chambers and veterans who participated as human subjects in WWI and postwar studies (8). The long-term effects on lungs were respiratory illnesses, including emphysema, chronic asthma, and chronic bronchitis (6, 9, 14–16). Furthermore, studies in Japan demonstrated high incidences of chronic respiratory complications, such as chronic bronchitis and lung cancer, in former workers of poison gas manufacturing factories that included SM, lewisite, and DPCA production for their use in WWII against China (6, 9, 17). Later, the soldiers from the Afghanistan–Iraq wars also had a high incidence of constrictive bronchiolitis associated with exposure to burn pits (18). Although facts show that lewisite exposure causes long-term respiratory complications, no research models are available to understand the underlying pathogenic mechanisms. DPCA-related long-term effects on developmental abnormalities, brain atrophy, and cerebral symptoms are known (19), and DPCA exposure–mediated long-term pulmonary effects are undocumented/unexplored.

Recently, our group has established a mouse model demonstrating that a single skin burn by lewisite (20, 21) or a less toxic degradation product of lewisite and DPCA, phenyl arsine oxide (PAO), results in acute lung injury (ALI) (21). In the present study, we have developed and characterized the long-term effects of skin exposure to sublethal doses of lewisite, DPCA, or PAO on the lungs of mice.

Methods

Detailed materials and methods are included in the data supplement.

Cutaneous Exposure to Lewisite and DPCA Exposure

All exposures to lewisite or DPCA were performed at the MRIGlobal facility under an approved animal protocol on adult male and female Ptch1$^{+/-}$/SKH-1 hairless mice (5–6 wk old). The dose of lewisite exposure was chosen based on the toxicity. This dose was sublethal dose for the Ptch1$^{+/-}$/SKH-1 hairless mice and did not cause death. The methods are included in the data supplement.

Statistical Analysis

Two-tailed *t* tests were performed for two-group comparisons and one-way ANOVA followed by Tukey's *post hoc* test for three or more group comparisons. A P value of <0.05 was considered significant. Values are shown as means ± SEM unless specified. All the statistical analyses were performed using GraphPad Prism 9.

Results

A Single Cutaneous Exposure of Lewisite and DPCA Causes Abnormalities in Mouse Lungs

We previously demonstrated that the single-dose application of lewisite and PAO on the skin causes ALI in mice (21). To further assess the long-term effects of cutaneous exposure of these arsenicals on the lungs, we analyzed the lungs of control and arsenical-exposed mice at 10 and 20 weeks after exposure by micro–computed tomography (micro-CT). The cross-section images of lewisite- and DPCA-exposed mouse lungs demonstrated the presence of increased opacities, a signature of increased inflammation or fibrosis in the lungs (Figure 1A). At 10 weeks after exposure, the lungs from the exposed group showed significantly increased mean lung density ($P < 0.001$) and hyperinflated lungs, showing increased total lung volumes relative to controls ($P < 0.001$) (Figures 1B and 1C). Our continued observations by micro-CT scans in the 20th week showed that the lungs of lewisite- and DPCA-exposed mice showed reduced numbers and intensity of opaque areas. However, more consolidated areas were observed around the airways (arrows in Figure 1D). Similarly, lewisite- and DPCA-exposed mice presented a significant difference in the mean lung density compared with control mice (Figure 1E). Lung hyperinflation demonstrated by increased total lung volume (Figure 1F; $P < 0.001$) was persistent in the exposed mice compared with control mice. Overall, progressive anatomical changes of the lung architecture from baseline were observed in micro-CT projections at 10 and 20 weeks after arsenical exposure in mice.

Single Cutaneous Exposure to Lewisite and DPCA Leads to Abnormal Lung Function Consistent with Constrictive Bronchiolitis

Next, we tested the lung function capacity of the lungs in control, lewisite, and DPCA groups. There were no significant changes in total lung compliance at 10 weeks after exposure in the lewisite and DPCA groups (Figure 2A). However, Newtonian resistance of central airways was increased in lewisite- and DPCA-exposed mice relative to control mice (Figure 2B). Although increased bronchial hyperreactivity was observed in lewisite- and DPCA-exposed mice compared with control mice (Figure 2C), there were no significant changes in total lung compliance at this time point (Figure 2D). The baseline increase in Newtonian resistance was observed in the lewisite and DPCA groups at the 20th week (Figure 2E). Mice in lewisite and DPCA groups continued to show increased hyperreactivity at the 20th week. The DPCA-exposed mice demonstrated higher airway resistance than the lewisite-exposed mice at higher doses

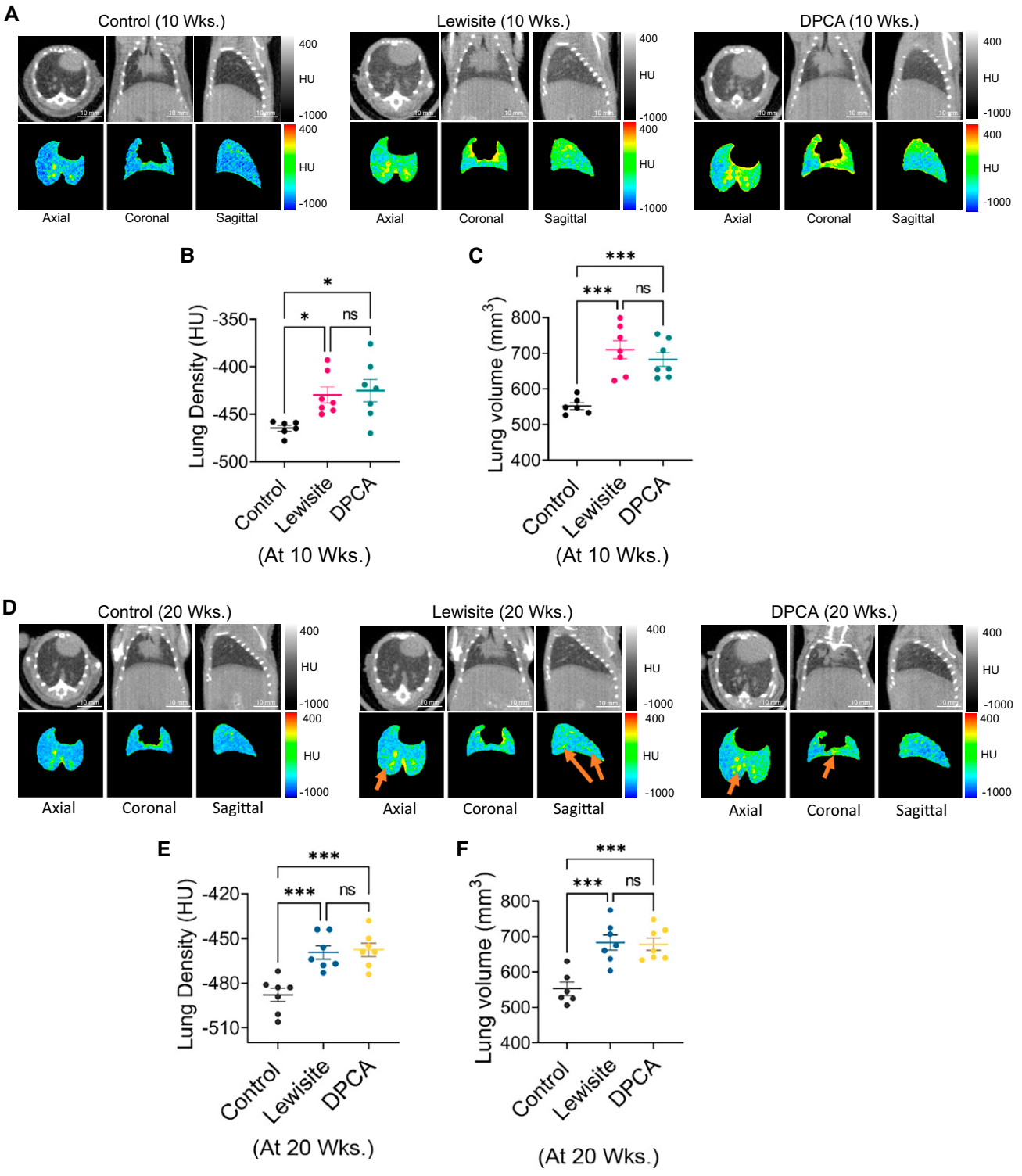

Figure 1. Cutaneous exposure to lewisite and di-phenyl chloro arsine (DPCA) causes long-term effects on lungs in mice. A single dose of lewisite (5 mg/kg body weight in 150 μl ethanol) or DPCA (equimolar amount of 5/mg kg body weight lewisite in 150 μl ethanol) was applied on dorsal skin of mice. (*A*) Representative micro–computed tomography (micro-CT) imaging axial, coronal, and sagittal projections of lungs of vehicle-, lewisite-, and DPCA-exposed mice at 10 weeks. (*B*) Mean lung density and (*C*) total lung volume in control, lewisite, and DPCA groups at 10 weeks. (D) Representative micro-CT imaging axial, coronal, and sagittal projections of lungs of vehicle-, lewisite-, and DPCA-exposed mice at 20 weeks. (*E*) Mean lung density and (*F*) total lung volume in control, lewisite, and DPCA groups at 20 weeks. The data are shown as mean ± SE; $n = 6$–10 per group. *$P < 0.05$ and ***$P < 0.001$ versus control group. One-way ANOVA was performed, followed by the Tukey *post hoc* test. HU = Hounsfield units; ns = not significant; Wks. = weeks. Scale bars, 10 mm.

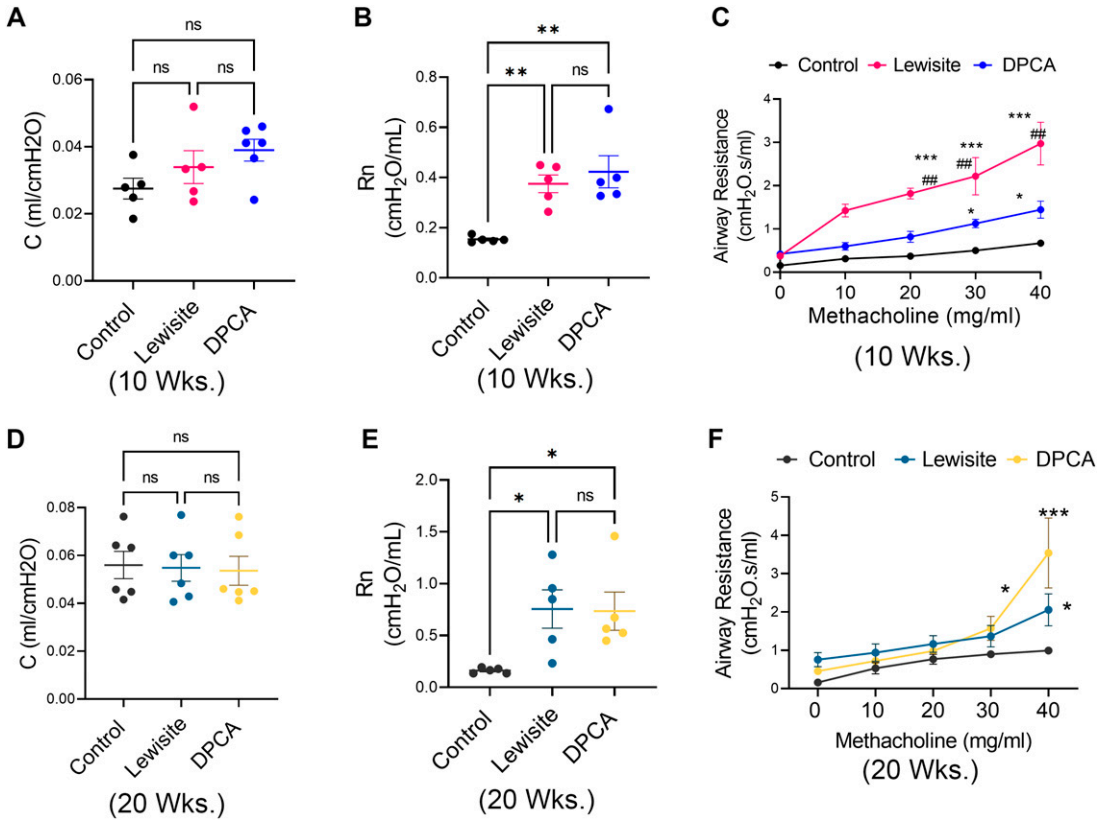

Figure 2. Cutaneous exposure to lewisite/DPCA increases airway resistance in mice. Respiratory mechanics analysis of lewisite/DPCA-exposed mice at 10 and 20 weeks. (*A*) Baseline values for compliance (C) and (*B*) Newtonian resistance (Rn) in control, lewisite, and DPCA mouse groups at 10 weeks. (*C*) Airway hyperreactivity assessments at different concentrations of methacholine in control, lewisite, and DPCA mouse groups at 10 weeks. (*D*) Baseline values for *C* and (*E*) Rn in control, lewisite, and DPCA mouse groups at 20 weeks. (*F*) Airway hyperreactivity assessments at different concentrations of methacholine in control, lewisite, and DPCA mouse groups at 10 weeks. Each dot represents an individual mouse. (*A*), (*B*), (*D*), and (*E*), $^{*}P < 0.05$, and $^{**}P < 0.01$ using one-way ANOVA followed by Tukey's *post hoc* analysis. (*C*) and (*F*), $^{*}P < 0.05$ and $^{***}P < 0.001$ versus controls and $^{\#\#}P < 0.01$, using two-way ANOVA. $n = 5$–6, each group.

of methacholine ($P < 0.05$) (Figure 2F). Overall, these results demonstrate decreased compliance and airway-related dysfunction in the lungs of lewisite- and DPCA-exposed mice.

Single Cutaneous Exposures to Lewisite and DPCA Cause Pathological Features of Constrictive Bronchiolitis

We compared micro-CT scan analysis to histological examination of the lungs in the control, lewisite, and DPCA groups. The hematoxylin and eosin–stained lung sections demonstrated that the Lewisite and DPCA groups had increased lung inflammation at 10 weeks after exposure. The lung inflammation subsided by the 20th week compared with the 10th week in the lewisite and DPCA groups (Figure 3A). However, we observed prominent airway remodeling in the arsenical-exposed mice at the 20th week (Figure 3A, insets). Furthermore, we observed that the bronchioles were obstructed with cellular mass and narrowed by excessive hyperplasic subepithelial thickness in the lewisite- and DPCA-exposed mice at the 20th week (Figure 3B). To avoid the artifacts due to high inflammation at the 10th week, we chose the 20-week postexposure group for further histological characterization of the lungs from lewisite- and DPCA-exposed mice and found an increase in epithelium height thickness (Figure 3C) ($P < 0.05$) in the airways of the lewisite- and DPCA-exposed mice. These mice also demonstrated increased collagen 1 and occasional presence of the tertiary lymphoid follicles (TLFs) associated with airways, whereas the control mice did not show presence of TLFs (Figure 3D). The airways of arsenical-exposed mice were surrounded with an increased number of $CD3^{+}$ T cells (Figures 3E and 3F). Thus, the single cutaneous exposure to lewisite or DPCA induced aberrant airway remodeling with the presence of lymphocyte-predominant inflammation.

Mice Exposed to a Single Cutaneous Exposure to Lewisite and DPCA Have Remodeled Airways

With our observations of inflamed and obstructed small airways and bronchioles, we further performed histological examination for extracellular matrix (ECM) deposition and α-SMA^{+} (alpha smooth muscle actin) cell hyperplasia and proliferation around the airways. Excessive increase in the collagen content of the airway wall was evident in the mice exposed to lewisite and DPCA (Figure 4A). Interestingly, the hydroxyproline contents of the whole lungs were elevated in the lewisite-exposed mice at 10 weeks after exposure (Figure 4B), which was further increased ($P < 0.05$) at Week 20. The DPCA-exposed mice demonstrated similar results ($P < 0.05$, 10th week vs. 20th week) (Figure 4C). α-SMA^{+} fibrotic

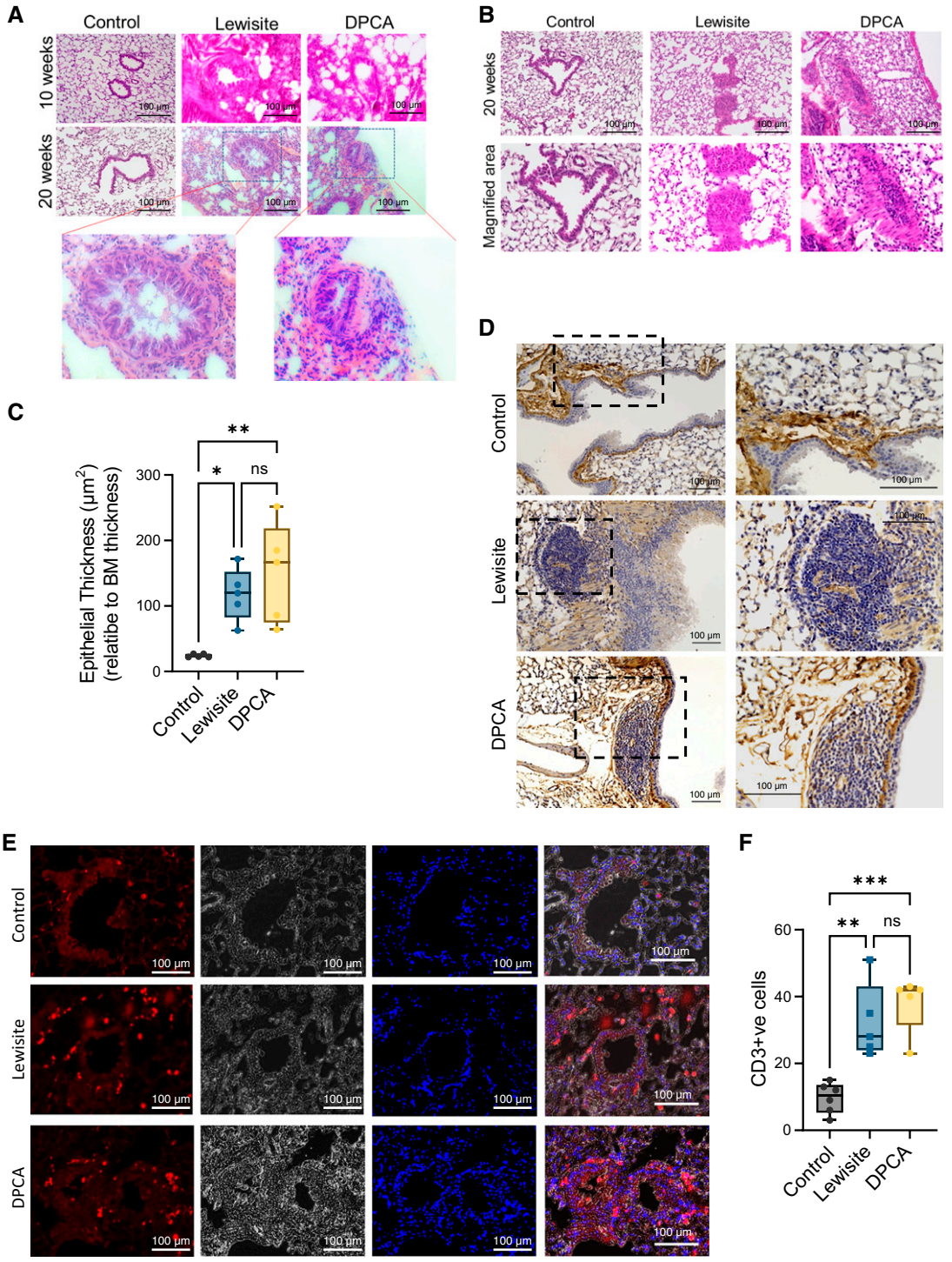

Figure 3. Cutaneous exposure to lewisite/DPCA causes constrictive bronchiolitis in mice. (*A*) Histopathological assessment of lung sections stained with hematoxylin and eosin at Weeks 10 and 20. Scale bars, 100 μm. Inset showing airway remodeling in lewisite and DPCA mouse groups at 20 weeks. Scale bars, 100 μm. (*B*) Small airways showing obstruction with growing cellular mass inside the airways. Scale bars, 100 μm. (*C*) Measurements of epithelial thickness of airways at 20 weeks. The line within the box represents the median. $^{*}P < 0.05$ and $^{**}P < 0.01$ versus control; *P* values were determined using one-way ANOVA with *post hoc* Tukey's method. $n = 5$–6, each group. (*D*) Representative images showing presence of tertiary lymphoid follicles next to the airways in the anti–collagen 1–stained lung sections in lewisite and DPCA groups at 20 weeks. Scale bars, 100 μm. (*E*) Immunofluorescence staining of lung sections for anti-CD3 (Alexa-594, red) and counterstain for nucleus (DAPI, blue) in control, lewisite, and DPCA groups at 20 weeks. Scale bars, 100 μm. (*F*) Quantitation of $CD3^{+}$ cells around airways. In box and whisker plots, box represent interquartile range, whiskers are extreme values, and dots show data points for individual mice. The line within the box represents the median. $^{**}P < 0.01$ and $^{***}P < 0.001$ versus control; *P* values were determined using one-way ANOVA with *post hoc* Tukey's method. $n = 5$–6, each group. BM = basement membrane; ns = not significant.

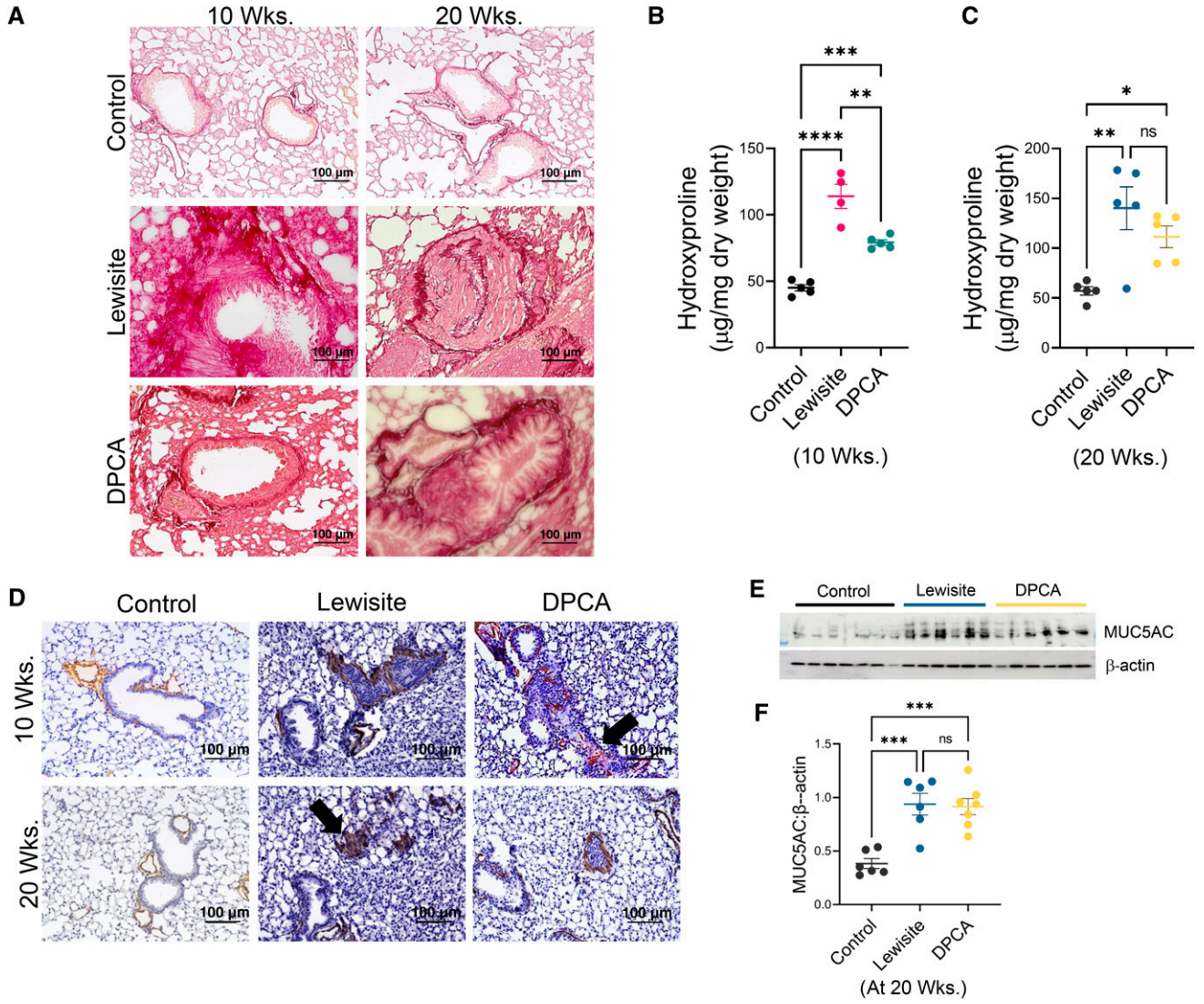

Figure 4. Cutaneous exposure to lewisite/DPCA causes airway remodeling in mice. (*A*) Representative lung histology with Picrosirius staining showing collagen deposition around airways at Weeks 10 and 20. Scale bars, 100 μm. (*B*) Hydroxyproline content at 10 weeks. (*C*) Hydroxyproline content at 20 weeks. (*D*) Representative lung histology with α-SMA (alpha smooth muscle actin) staining at Weeks 10 and 20. Scale bars, 100 μm. (*E*) Immunoblot analysis in whole lung tissue lysates for MUC5AC (mucin 5 AC). β-actin expression was used as loading control. (*F*) Densitometry of MUC5AC expression. Each dot represents an individual mouse. $^{*}P < 0.05$, $^{**}P < 0.01$, and $^{***}P < 0.001$ using one-way ANOVA followed by Tukey's *post hoc* analysis.

and hypertrophic areas around airways were observed in lewisite- and DPCA-exposed mice at both time points (Figure 4D). In addition, we observed that the small airways were obstructed with α-SMA^{+} fibrotic scars (black arrows) in lewisite-exposed mice at the 20th week (Figure 4D). Furthermore, during the histopathological examinations, we did not observe the specific pattern for the involvement of a particular lobe of the lung. The disease was heterogeneous, and constriction of airways was present in the random lobe/lobes.

Increased hyperresponsiveness of the airways is suggestive of airway inflammation and uncleared mucus. Hence, we assessed the expression of Muc5AC (Mucin 5AC) in the lungs of these mice (Figures 4E and 4F). There was a significant increase in the expression of Muc5AC at the 20th week ($P < 0.01$) relative to the control mice (Figure 4F). We did not observe the expression of Muc5AC at the 10th week after exposures (data not shown). Overall, the pathological features of constrictive bronchiolitis, such as the presence of excessive matrix, smooth-muscle hypertrophy around bronchioles, and increased MUC5AC production, were observed in the mice cutaneously exposed to lewisite and DPCA.

PAO Mimics Characteristics of Lewisite-inflicted Long-Term Effects on Mouse Lungs

PAO, a less toxic and surrogate chemical to lewisite, induces ALI after a single cutaneous exposure (21, 22). We tested if it can also result in long-term effects on the lungs. The single cutaneous exposure to PAO led to increased opacities in the cross-section

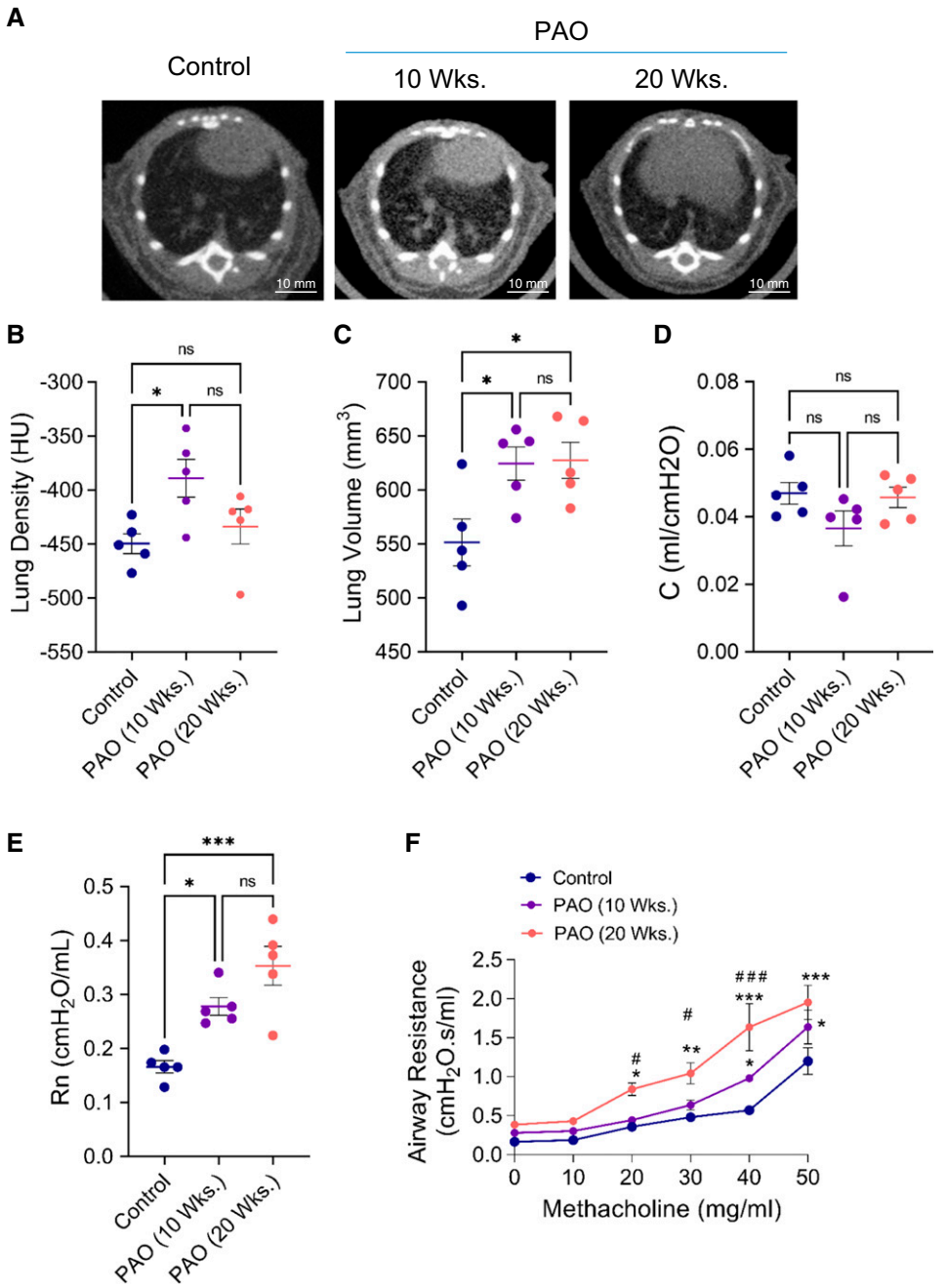

Figure 5. Exposure to PAO (phenyl arsine oxide) on skin causes long-term effects in the lungs of mice. PAO (200 μg in 150 μl ethanol), a surrogate chemical to lewisite, was applied on the dorsal skin. Micro-CT scan and lung functions were analyzed at Weeks 10 and 20 after exposure. (*A*) Representative micro-CT imaging image of lungs of vehicle- and PAO-exposed mice at Weeks 10 and 20. Scale bars, 10 mm. (*B*) Mean lung density and (*C*) total lung volume in control and PAO groups at 10 and 20 weeks. (*D*) Baseline values for compliance (C) and (*E*) Newtonian resistance (Rn) in control and PAO mouse groups at 10 and 20 weeks. (*F*) Airway hyperreactivity assessments at different concentrations of methacholine in control and PAO mouse groups at 10 and 20 weeks. (*B*), (*C*), (*D*), and (*E*), $^{*}P<0.05$ and $^{**}P<0.01$ using one-way ANOVA followed by Tukey's *post hoc* analysis. (*F*), $^{*}P<0.05$, $^{**}P<0.01$, and $^{***}P<0.001$ versus control mice, and $^{\#}P<0.05$ and $^{\#\#\#}P<0.001$ for PAO 10 weeks versus PAO 20 weeks, using two-way ANOVA. $n=5$–6, each group.

micro-CT images of the lungs at 10 and 20 weeks after exposure (Figure 5A). However, mean lung density was increased at the 10th week, and there was no significant difference in the mean lung density at the 20th week (Figure 5B). Interestingly, PAO exposure increased lung volumes at both time points (Figure 5C). We next analyzed if PAO-exposed mice showed any effect on lung function. We observed no significant changes in lung compliance (Figure 5D) compared with the control mice. Baseline

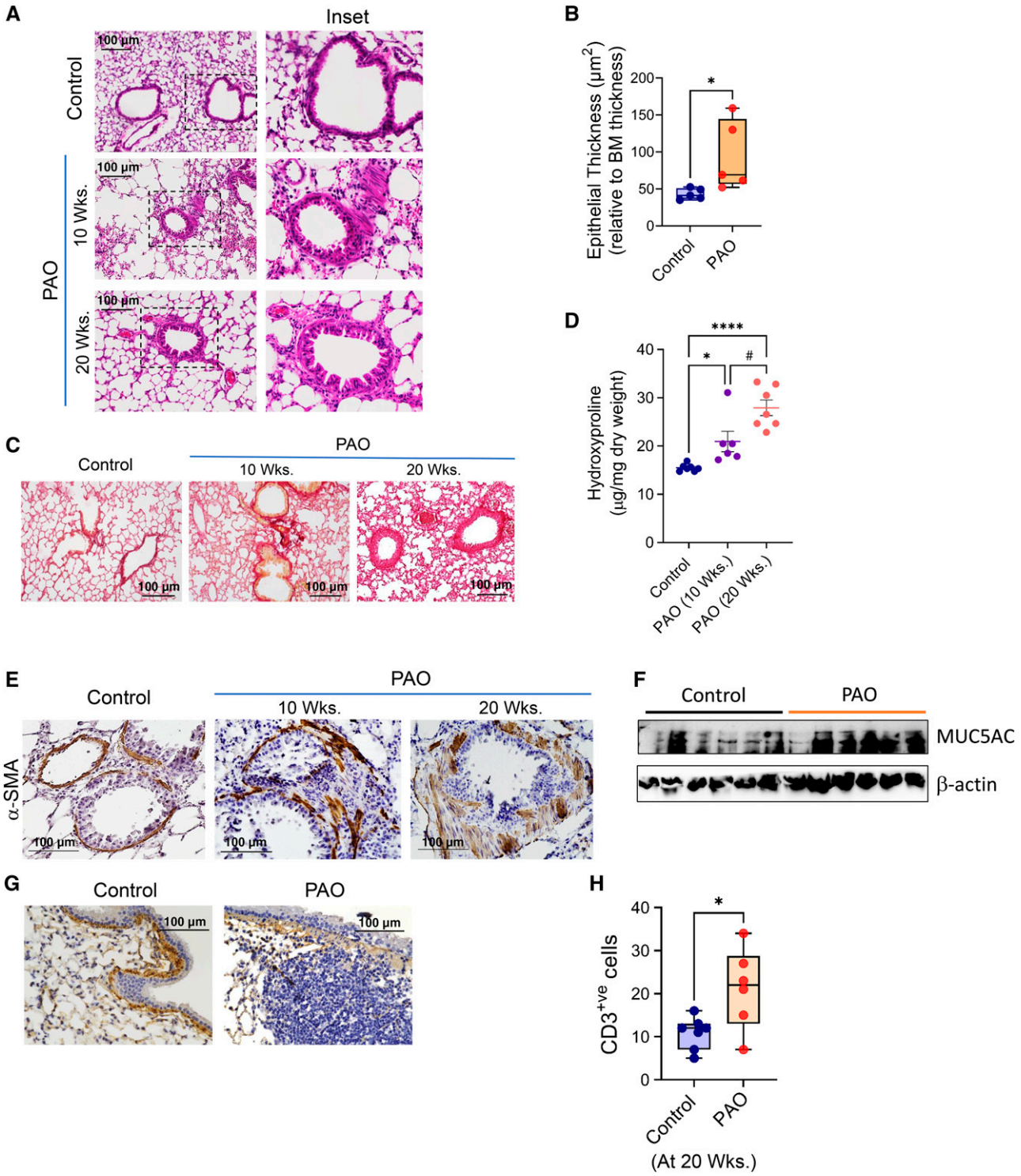

Figure 6. Cutaneous exposure to PAO causes constrictive bronchiolitis. (*A*) Histopathological assessment of lung sections stained with hematoxylin and eosin from vehicle- and PAO-exposed mice at Weeks 10 and 20. Scale bars, 100 μm. Inset showing airway remodeling in PAO mouse groups. (*B*) The measurements of epithelial thickness of airways at 20 weeks. (*C*) Picrosirius staining showing collagen deposition around airways at Weeks 10 and 20. Scale bars, 100 μm. (*D*) Hydroxyproline content of whole lung. (*E*) Representative lung histology with α-SMA staining at Weeks 10 and 20. Scale bars, 100 μm. (*F*) Immunoblot analysis in whole lung tissue lysates for MUC5AC. β-actin expression was used as loading control. (*G*) Representative images showing presence of tertiary lymphoid follicles next to the airways in the anti–collagen 1–stained lung sections at 20 weeks. Scale bars, 100 μm. (*H*) Quantitation of $CD3^+$ cells around airways. In box and whisker plots, box represent interquartile range, whiskers are extreme values, and dots show data points for individual mice. Lines within the boxes represent the median. $^*P < 0.05$ and $^{****}P < 0.0005$ versus control; $^{\#}P < 0.05$ PAO 10 weeks versus PAO 20 weeks. *P* values were determined using one-way ANOVA with *post hoc* Tukey's method. $n = 5$–6, each group.

airway resistance was increased in PAO-exposed mice at both time points compared with control mice (Figure 5E). Furthermore, the PAO-exposed mice demonstrated increased airway resistance at higher doses of methacholine treatment compared with the control group (Figure 5F). The Airway hyperreactivity was significantly increased in 20-week PAO-exposed mice as compared with 10-week PAO-exposed mice at different doses of methacholine (here, $^{\#}P < 0.05$ is 10-weeks after PAO versus 20-weeks after PAO at methacholine challenge at the dose of 20 and 30 mg/ml, and $^{\#\#\#}P < 0.001$, 10-weeks after PAO versus 20-weeks after PAO at methacholine challenge at the dose of 40 mg/ml). Thus, we observed that single-dose cutaneous exposure to PAO decreased lung function in mice in the 10th and 20th weeks.

Single Cutaneous Exposure to PAO Causes Constrictive Bronchiolitis as a Long-term Effect in Mouse Lungs

Hematoxylin and eosin staining demonstrated increased inflammation in the lungs of PAO-exposed mice at the 10th and 20th weeks. The inset in Figure 6A demonstrates the increased airway remodeling in the PAO-exposed mice. Cutaneous exposure to PAO increased

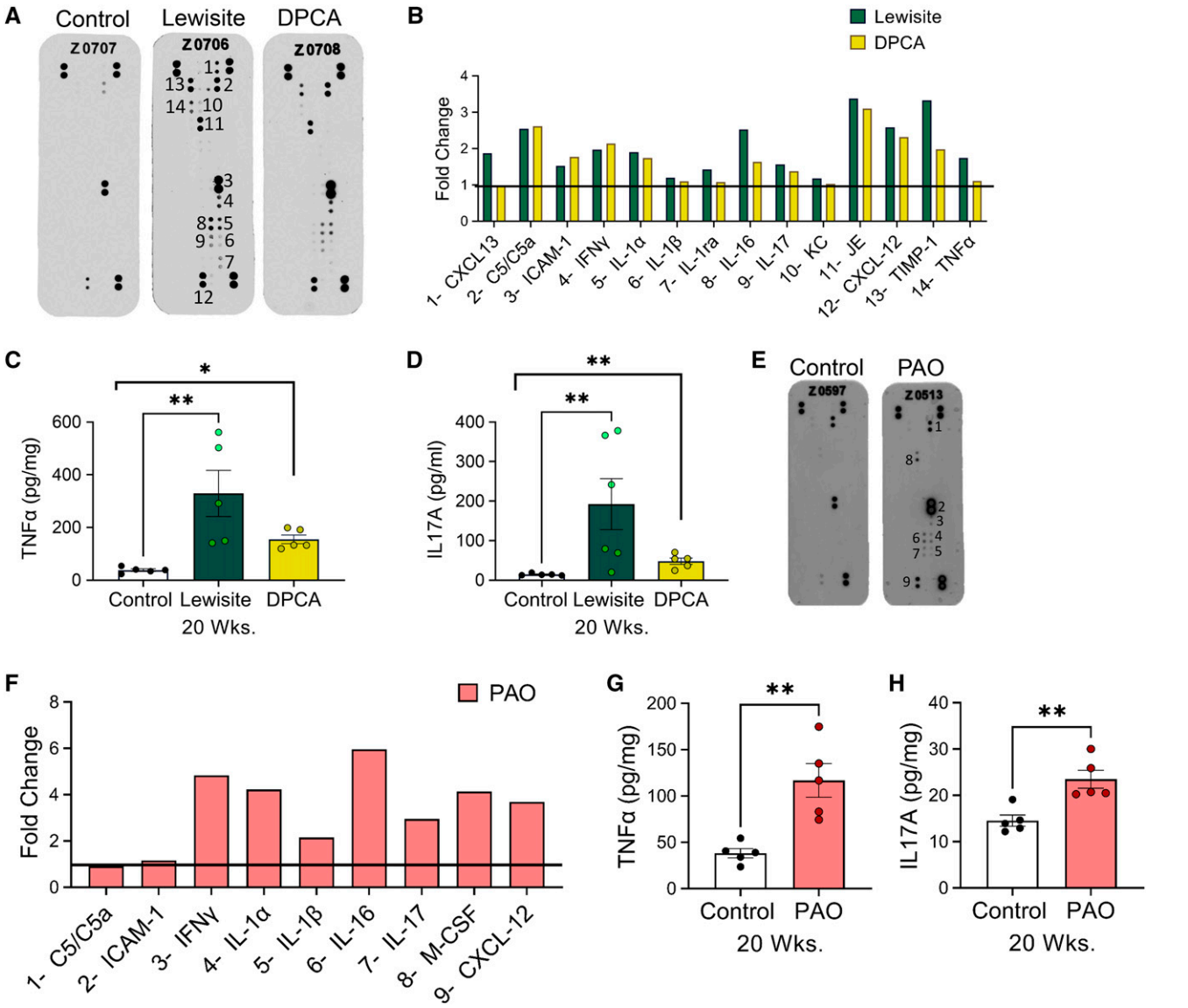

Figure 7. (*A*) Mouse cytokine antibody array showing expression patterns of different cytokines in serum samples of vehicle control-, lewisite-, and DPCA-exposed mice, and (*B*) graph showing relative fold change induction of proinflammatory cytokines compared with control mice at 20 weeks. (*C*) TNF-α (tumor necrosis factor α) and (*D*) IL-17A ELISA in lung lysates at 20 weeks. (*E*) Antibody microarray and (*F*) its densitometry graph from the serum samples from PAO-exposed mice at 20 weeks. (*G*) TNF-α and (*H*) IL-17A protein levels in the lung lysates from control mice and PAO group at 20 weeks after exposure. In (*A*), (*B*), (*E*), and (*F*), the number on the microarray image matches the number in front of the cytokine name on the *x*-axis of the graph. In these experiments, serum samples of three mice from each group were pooled and incubated with a mouse cytokine antibody array membrane. Densitometry data obtained from the array images were analyzed by National Institutes of Health ImageJ software and presented as the fold changes normalized with control mouse group. (*C*), (*D*), (*G*), and (*H*), $n = 5$ mice/group. $^{*}P < 0.05$ and $^{**}P < 0.01$, arsenical versus control, using individual Student's *t* tests.

epithelial thickness of the airways compared with control mice at 20 weeks (Figure 6B). Furthermore, immune-histological assessment for collagen deposition by Picrosirius staining and α-SMA staining demonstrated increased thickness of collagen and α-SMA$^+$ peribronchial fibrosis (Figures 6C and 6E, respectively). The overall content for hydroxyproline was enhanced in PAO-exposed mice (Figure 6D). PAO-exposed mice demonstrated increased MUC5AC production at the 20th week (Figure 6F). Cutaneous exposure to PAO demonstrated an increase in lymphocytic inflammation by the 20th week around the airways. We observed the presence of TLFs (Figure 6G) and increased numbers of CD3$^+$ T-helper cells around the airways (Figure 6H) in PAO-exposed mice at the 20th week. Collectively, these findings suggest that PAO skin exposure causes *in vivo* lung airway remodeling, especially by induction of excessive collagen 1–rich ECM production, and α-SMA deposition around the airways with the presence of lymphocytic inflammation.

Single Cutaneous Exposure to Lewisite, DPCA, and PAO Instigates Systemic and Lung Inflammation

We tested serum samples by a cytokine microarray of the serum from lewisite- and DPCA-exposed mice, which at 20 weeks demonstrated fold change normalized with the control mice for the expression of CXCL-13, C5/C5a (complement component 5a), ICAM-1 (intercellular adhesion molecule 1), IFNγ, IL-1α, IL-1β, IL-16, IL-17, KC (keratinocyte chemoattractant) (CXCL-1), JE (mouse homolog for MCP-1) (CCL2/MCP1 [monocyte chemoattractant protein-1]), CXCL-12, TIMP-1 (tissue inhibitor of metalloproteinases), and TNF-α. Furthermore, lewisite exposure demonstrated higher amounts of inflammatory cytokines IL-1β, IL-1ra, IL-16, IL-17, KC, JE, CXCl2, TIMP-1, and TNF-α (tumor necrosis factor) compared with DPCA-exposed mice (Figures 7A and 7B). Because of the presence of CD3$^+$ cells in lungs, we tested for levels of TNF-α and IL-17A by ELISA. A single cutaneous exposure to lewisite and DPCA increased levels of TNF-α (Figure 7C) and IL-17A (Figure 7D) in lungs. Similar to lewisite and DPCA, the microarray demonstrated increased levels of ICAM-1, IFNγ, IL-1α, IL-1β, IL-1ra, IL-16, M-CSF (macrophage colony-stimulating factor), and CXCL-12 (Figures 7E and 7F). The levels of TNF-α and IL17A were increased in mice exposed to PAO at 20 weeks. Lung lysates demonstrated significantly increased protein levels of TNF-α (Figure 7G) and IL-17A (Figure 7H) in lewisite, DPCA, and PAO mouse groups at 20 weeks.

Discussion

The U.S. Department of Veterans Affairs has identified that lewisite exposure can cause long-term effects (23), including developing chronic forms of bronchitis, emphysema, asthma, or chronic obstructive pulmonary disease. The Iranian survivors of SM exposure developed chronic bronchitis (24, 25). Several retrospective studies show the prevalence of constrictive bronchiolitis in veterans who served in military operations (18, 26, 27). The direct causative agents for these long-term effects are not known. Because of the lack of appropriate animal models, understanding molecular mechanisms for the pathogenesis of these diseases is limited. For the first time, in this study, we have developed a mouse model that recapitulates the physiological and pathological features of constrictive bronchiolitis as a long-term pulmonary toxicity after a single cutaneous lewisite exposure.

We recently demonstrated that severe skin burns by lewisite or PAO resulted in ALI in mice (20, 21). Per our observations (20, 21) and those of others (11), we found that the mice exposed to lewisite and DPCA had inflammation after 24 hours (*see* Figure E1 in the data supplement). The acute inflammation subsided moderately by 10 weeks after exposure (Figure 1); however, the prominent remodeling of airways with characteristic pathological signs of constrictive bronchiolitis was noted at 20 weeks after exposure. Our mouse model recapitulates the pathology and disease progression in chemical plant workers and veterans exposed to lewisite (8).

The micro-CT scans of the lungs of these arsenical-exposed mice demonstrated increased mean lung densities and lung volumes relative to control mice at 10 weeks after exposure. Increased mean densities of lungs indicated the presence of either inflammation or fibrosis. Human survivors of acute respiratory distress syndrome also demonstrate the presence of interstitial ground-glass opacities (28). We observed increased densities that were due to the influx of inflammatory cells in the lungs. Furthermore, regardless of recovery in terms of lung volumes 6 months after acute respiratory distress syndrome in patients, there is a decrease in diffusing capacity and abnormal lung function 5 years after recovery (29). We found constricted or blocked airways in the histological analysis and high airway resistance during methacholine challenge in mice that may be responsible for the lower diffusing capacity and resulting larger lung volumes. Furthermore, micro-CT scans in the exposed mice also revealed that mean lung density was reduced to comparable levels to control mice by 20 weeks after exposure, but the lung volumes remained higher (Figure 1). These observations resemble the accepted features of constrictive bronchiolitis, with inflammation and/or fibrosis around the airways, sparing parenchymal involvement (30, 31) and hyperinflation of lungs (32, 33). Patients with constrictive bronchiolitis have hyperinflation of the lungs due to limited airflow (27). SM-exposed human survivors also demonstrate air trapping in the lungs (24), increased airway resistance, and hyperreactivity-evidenced airflow obstruction. Similar findings in our experimental mice are possibly responsible for increased lung volumes in the lewisite-, DPCA-, and PAO-exposed groups.

Constrictive bronchiolitis typically presents with intraluminal or peribronchiolar fibrosis ranging from the proliferation of fibroblasts and myofibroblasts to collagen deposition and scarring (18, 34, 35). By histologic and quantitative morphometric analysis, we observed similar pathological abnormalities, including collagen scarring in the peribronchiolar regions in mice exposed to arsenicals. The collagen scarring around the airways became more evident by 20 weeks after exposure. The association between the total collagen content of lungs and the severity of constrictive bronchiolitis needs to be established because of the limited human samples for research and the lack of reproducible animal models. However, the increased levels of newly formed collagen 1 in BAL were positively correlated with the progression of the closely similar clinical disease called bronchiolitis obliterans syndrome (36). The enhanced pathological collagen scarring around the airways confers greater strength and stiffness (37), thereby suggesting the intensifying of

airway resistance and hyperresponsiveness at 20 weeks after exposure to arsenicals compared with 10 weeks after exposure. The increased adventitial thickness with the presence of α-SMA$^+$ cells demonstrated the hypertrophy of myofibroblasts around the airway that progressed to total closure of small airways with the α-SMA$^+$ fibrotic scars. It suggests that these obliterated airways cause a decrease in airflow, resulting in decreased compliance, a common manifestation of constrictive bronchiolitis obliterans (33). Moreover, we observed no significant increase in the collagen content and peribronchiolar fibrosis after 30 weeks of exposure to lewisite and DPCA (Figure E2). These observations agree with the literature suggesting that the disease severity of airway diseases is associated with airway remodeling but not the length of disease (38).

In veterans, deployment-related constrictive bronchiolitis demonstrates lymphocytic airway inflammation (26). Specifically, the lung tissue biopsies from civilians and military personnel from the Iran–Iraq War who survived after exposure to SM demonstrated the presence of lymphocytic infiltrates in the lungs (24). We observed increased numbers of tertiary lymphoid follicles around airways in lewisite- and DPCA-exposed mice, which showed similarities with the features observed in lung biopsies from military personnel and veterans with constrictive bronchiolitis (26). TLFs are not a constitutive feature of healthy human lungs, and lymphoid neogenesis is a feature of inflammatory conditions. However, their functions have yet to be described adequately. They may have a circumferential presence and may not have a role in developing bronchiolitis obliterans (39). Some studies suggest that degradation products of ECM and cell death due to inflammation generate self-antigens that stimulate the neogenesis of TLFs. Further studies are necessary to elucidate their role in constrictive bronchiolitis.

T cells and lymphocytes in constrictive bronchiolitis are consistently present in the survivors of SM exposure in Iran with constrictive bronchiolitis (40). Moreover, the development and severity of constrictive bronchiolitis in patients with lung transplant rejection are also associated with increased T cells (41). Specifically, CD4$^+$ T cells have an active role in epithelial injury and are known to contribute to persistent inflammation and fibrosis in constrictive bronchiolitis after lung transplantation (42). The closely related rat model of bronchiolitis obliterans after inhalation injury using SM and diacetyl demonstrated chronic inflammation and activation of T cell immune response in rat lungs (43, 44). We observed the similarities in adaptive T cell response in our mouse model of constrictive bronchiolitis. Lewisite and DPCA increased T cell activity–related cytokines IL-16, IL-17, IL-1a, and IL-1β that are identified for their role in constrictive bronchiolitis (26, 45).

Complement activation is a critical factor in the inflammatory immune response in transplant rejection. However, the absence of a complement response can also show the development of obliterated airway disease for chronic lung rejection (46). Interestingly, DPCA and lewisite increased complement activation; however, PAO-exposed mice demonstrated no effect on C5/C5a levels. Furthermore, the PAO-exposed mice, similar to lewisite and DPCA mice, demonstrated increased expression of GM-CSF, IFNγ, IL-1a, IL-1β, IL-16, and IL-17, which points toward increased dendritic cells and T cell activity, which is a recognized feature of allograft rejection (47, 48). Patients with SM exposure (40) and relevant experimental models, such as subcutaneous injection of SM in mice (49) and the bronchiolitis obliterans model in rats by the inhalation of diacetyl, also demonstrate increased T cell activation (44). The increased levels of CXCL-12 in lewisite-, DPCA-, and PAO-exposed mice can be associated with the activation of CD8 T cells known to contribute to allograft rejection (50). Overall, the increased T cell activation is similar to the immunopathology observed in soldiers with postdeployment constrictive bronchiolitis (26).

Chronic airway diseases are associated with mucus hypersecretion (51, 52). We observed the T cell population increase around the airways at 20 weeks after exposure. We observed a significant increase in the expression of Muc5AC at 20 weeks after exposure to arsenicals (Figures 4 and 6). Interestingly, the increased expression of Muc5AC was not detected at 10 weeks after exposure. A plausible explanation is that the decreased inflammation and the repair processes induce mucus secretion by the 20th week (53). Increased levels of T cell activity and IL-17A in lungs of arsenical-exposed mice at the 20th week can be responsible for increased secretion of Muc5AC (54).

In conclusion, we have established a novel mouse model of small airway remodeling that represents the pathological features observed in constrictive bronchiolitis, specifically in military personnel and veterans. Around 50% of survivors of the Iran War develop constrictive bronchiolitis and similar airway diseases (24). The chronic pulmonary toxicity of vesicant injury is largely dependent on adaptive immunity and T cell activation. Compared with a previously described model of SM inhalation, nose-only inhalation resulted in severe nasal epithelial degeneration but minimal lung injury in up to 6 days (55); however, the application of SM subcutaneously clearly demonstrated increased systemic T cell activity in 7 days (49). We studied our model for a longer period of time and continued to observe increased T cell activity and the constriction of the airways at 20 weeks. Recent work for studying the chronic effects of diacetyl inhalation in the rat model has similar supportive observations (44). One limitation in the present study is that we did not perform arterial blood gas exchange studies in our model; however, the lung mechanics clearly supported the histopathological observations. We anticipate that the constriction of airways will lead to decreased arterial blood gas exchange, as found in obstructive airway diseases (56) and a diacetyl model of bronchiolitis obliterans in rats at Day 19 (44). Our study provides the quintessential characteristics of constrictive bronchiolitis in a small animal model without requiring toxic inhalation or major airway manipulation like graft-versus-host disease (GVHD) models of constrictive bronchiolitis (57). Further in-depth research on these mechanisms will benefit the medical and veteran communities by understanding the pathogenesis of constrictive bronchiolitis and discovering targets for novel therapy. ■

Author disclosures are available with the text of this article at www.atsjournals.org.

Acknowledgment: The authors thank Weng Zhiping for communication assistance with MRIGlobal for the lewisite and DPCA exposure experiments. The authors thank Samuel Sharon for her assistance with micro-CT scans of the animals.

References

1. Goldman L, Cullen GE. The vesicant chemical warfare agents. *Arch Derm Syphilol* 1940;42:123–136.
2. Abbas F. Report of the specialists appointed by the Secretary-General of the United Nations to investigate allegations by the Islamic Republic of Iran concerning the use of chemical weapons. *Arch Belges* 1984; 302–310.
3. Vaezihir A, Pirkhezranian A, Sehati N, Hosseinzadeh MR, Salehi-Lisar SY, Sanderson H. Investigation of long-term hazards of chemical weapon agents in the environment of Sardasht area, Iran. *Environ Sci Pollut Res Int* 2022;29:498–508.
4. Kadivar H, Adams SC. Treatment of chemical and biological warfare injuries: insights derived from the 1984 Iraqi attack on Majnoon Island. *Mil Med* 1991;156:171–177.
5. Isono O, Kituda A, Fujii M, Yoshinaka T, Nakagawa G, Suzuki Y. Long-term neurological and neuropsychological complications of sulfur mustard and Lewisite mixture poisoning in Chinese victims exposed to chemical warfare agents abandoned at the end of WWII. *Toxicol Lett* 2018;293:9–15.
6. Nishimoto Y, Burrows B, Miyanishi M, Katsuta S, Shigenobu T, Kettel LJ. Chronic obstructive lung disease in Japanese poison gas workers. *Am Rev Respir Dis* 1970;102:173–179.
7. Tewari-Singh N, Goswami DG, Kant R, Ammar DA, Kumar D, Enzenauer RW, *et al.* Histopathological and molecular changes in the rabbit cornea from arsenical vesicant lewisite exposure. *Toxicol Sci* 2017;160:420–428.
8. Institute of Medicine (US) Committee on the Survey of the Health Effects of Mustard Gas and Lewisite. Nonmalignant respiratory effects of mustard agents and lewisite. In: Rall DP, Pechura CM, editors. *Veterans at risk: the health effects of mustard gas and lewisite*. Washington, DC: National Academies Press; 1993.
9. Nishimura Y, Iwamoto H, Ishikawa N, Hattori N, Horimasu Y, Ohshimo S, *et al.* Long-term pulmonary complications of chemical weapons exposure in former poison gas factory workers. *Inhal Toxicol* 2016;28:343–348.
10. Patocka J, Kuka K. Irritant compounds: military respiratory irritants. Part II. Sternutators. *Military Medical Science Letter* 2016;85:50–55.
11. Dekanski J. The pathology of phenyldichloroarsine poisoning in rabbits. *Br J Exp Pathol* 1948;29:39–47.
12. Bourassa S, Paquette-Raynard E, Noebert D, Dauphin M, Akinola PS, Marseilles J, *et al.* Gaps in prehospital care for patients exposed to a chemical attack: a systematic review. *Prehosp Disaster Med* 2022;37: 1–10.
13. Jett DA, Yeung DT. The CounterACT Research Network: basic mechanisms and practical applications. *Proc Am Thorac Soc* 2010;7: 254–256.
14. Amini H, Solaymani-Dodaran M, Mousavi B, Alam Beladi SN, Soroush MR, Abolghasemi J, *et al.* Long-term health outcomes among survivors exposed to sulfur mustard in Iran. *JAMA Netw Open* 2020;3:e2028894.
15. Graham JS, Schoneboom BA. Historical perspective on effects and treatment of sulfur mustard injuries. *Chem Biol Interact* 2013;206: 512–522.
16. Razavi SM, Ghanei M, Salamati P, Safiabadi M. Long-term effects of mustard gas on respiratory system of Iranian veterans after Iraq-Iran war: a review. *Chin J Traumatol* 2013;16:163–168.
17. Doi M, Hattori N, Yokoyama A, Onari Y, Kanehara M, Masuda K, *et al.* Effect of mustard gas exposure on incidence of lung cancer: a longitudinal study. *Am J Epidemiol* 2011;173:659–666.
18. King MS, Eisenberg R, Newman JH, Tolle JJ, Harrell FE Jr, Nian H, *et al.* Constrictive bronchiolitis in soldiers returning from Iraq and Afghanistan. *N Engl J Med* 2011;365:222–230.
19. Ishii K, Tamaoka A, Otsuka F, Iwasaki N, Shin K, Matsui A, *et al.* Diphenylarsinic acid poisoning from chemical weapons in Kamisu, Japan. *Ann Neurol* 2004;56:741–745.
20. Manzoor S, Mariappan N, Zafar I, Wei CC, Ahmad A, Surolia R, *et al.* Cutaneous lewisite exposure causes acute lung injury. *Ann N Y Acad Sci* 2020;1479:210–222.
21. Surolia R, Li FJ, Wang Z, Kashyap M, Srivastava RK, Traylor AM, *et al.* NETosis in the pathogenesis of acute lung injury following cutaneous chemical burns. *JCI Insight* 2021;6:e147564.
22. Li C, Srivastava RK, Athar M. Biological and environmental hazards associated with exposure to chemical warfare agents: arsenicals. *Ann N Y Acad Sci* 2016;1378:143–157.
23. U.S. Department of Veterans Affairs. Disability benefits: mustard gas or lewisite exposure. [accessed 15 Aug 2022]. Available from: https://www.va.gov/disability/eligibility/hazardous-materials-exposure/mustard-gas-lewisite/.
24. Ghanei M, Tazelaar HD, Chilosi M, Harandi AA, Peyman M, Akbari HM, *et al.* An international collaborative pathologic study of surgical lung biopsies from mustard gas-exposed patients. *Respir Med* 2008;102: 825–830.
25. Khateri S, Ghanei M, Keshavarz S, Soroush M, Haines D. Incidence of lung, eye, and skin lesions as late complications in 34,000 Iranians with wartime exposure to mustard agent. *J Occup Environ Med* 2003;45: 1136–1143.
26. Gutor SS, Richmond BW, Du RH, Wu P, Lee JW, Ware LB, *et al.* Characterization of immunopathology and small airway remodeling in constrictive bronchiolitis. *Am J Respir Crit Care Med* 2022;206: 260–270.
27. Banks DE, Bolduc CA, Ali S, Morris MJ. Constrictive bronchiolitis attributable to inhalation of toxic agents: considerations for a case definition. *J Occup Environ Med* 2018;60:90–96.
28. Herridge MS, Cheung AM, Tansey CM, Matte-Martyn A, Diaz-Granados N, Al-Saidi F, *et al.*; Canadian Critical Care Trials Group. One-year outcomes in survivors of the acute respiratory distress syndrome. *N Engl J Med* 2003;348:683–693.
29. Chiumello D, Coppola S, Froio S, Gotti M. What's next after ARDS: long-term outcomes. *Respir Care* 2016;61:689–699.
30. Swaminathan AC, Carney JM, Tailor TD, Palmer SM. Overview and challenges of bronchiolar disorders. *Ann Am Thorac Soc* 2020;17: 253–263.
31. Barker AF, Bergeron A, Rom WN, Hertz MI. Obliterative bronchiolitis. *N Engl J Med* 2014;370:1820–1828.
32. Edwards RM, Kicska G, Schmidt R, Pipavath SN. Imaging of small airways and emphysema. *Clin Chest Med* 2015;36:335–347, x.
33. McLoud TC. Occupational lung disease. *Radiol Clin North Am* 1991;29: 931–941.
34. Epler GR. Constrictive bronchiolitis obliterans: the fibrotic airway disorder. *Expert Rev Respir Med* 2007;1:139–147.
35. Zheng L, Ward C, Snell GI, Orsida BE, Li X, Wilson JW, *et al.* Scar collagen deposition in the airways of allografts of lung transplant recipients. *Am J Respir Crit Care Med* 1997;155:2072–2077.
36. Morrone C, Smirnova NF, Jeridi A, Kneidinger N, Hollauer C, Schupp JC, *et al.* Cathepsin B promotes collagen biosynthesis, which drives bronchiolitis obliterans syndrome. *Eur Respir J* 2021;57:2001416.
37. Liu L, Stephens B, Bergman M, May A, Chiang T. Role of collagen in airway mechanics. *Bioengineering (Basel)* 2021;8:13.
38. Bai TR, Cooper J, Koelmeyer T, Paré PD, Weir TD. The effect of age and duration of disease on airway structure in fatal asthma. *Am J Respir Crit Care Med* 2000;162:663–669.
39. Hodge G, Hodge S, Liu H, Nguyen P, Holmes-Liew CL, Holmes M. Bronchiolitis obliterans syndrome is associated with increased senescent lymphocytes in the small airways. *J Heart Lung Transplant* 2021;40:108–119.
40. Panahi Y, Ghanei M, Hassani S, Sahebkar A. TGF-β and Th17 cells related injuries in patients with sulfur mustard exposure. *J Cell Physiol* 2018;233:3037–3047.
41. Medoff BD, Seung E, Wain JC, Means TK, Campanella GS, Islam SA, *et al.* BLT1-mediated T cell trafficking is critical for rejection and obliterative bronchiolitis after lung transplantation. *J Exp Med* 2005; 202:97–110.
42. Zhu Z, Homer RJ, Wang Z, Chen Q, Geba GP, Wang J, *et al.* Pulmonary expression of interleukin-13 causes inflammation, mucus hypersecretion, subepithelial fibrosis, physiologic abnormalities, and eotaxin production. *J Clin Invest* 1999;103:779–788.
43. McGraw MD, Dysart MM, Hendry-Hofer TB, Houin PR, Rioux JS, Garlick RB, *et al.* Bronchiolitis obliterans and pulmonary fibrosis after sulfur mustard inhalation in rats. *Am J Respir Cell Mol Biol* 2018;58:696–705.
44. House EL, Kim SY, Johnston CJ, Groves AM, Hernady E, Misra RS, *et al.* Diacetyl vapor inhalation induces mixed, granulocytic lung inflammation with increased $CD4^{+}CD25^{+}$ T cells in the rat. *Toxics* 2021;9:359.

45. Laan M, Lindén A, Riise GC. IL-16 in the airways of lung allograft recipients with acute rejection or obliterative bronchiolitis. *Clin Exp Immunol* 2003;133:290–296.
46. Takenaka M, Subramanian V, Tiriveedhi V, Phelan D, Hachem R, Trulock E, *et al.* Complement activation is not required for obliterative airway disease induced by antibodies to major histocompatibility complex class I: implications for chronic lung rejection. *J Heart Lung Transplant* 2012;31:1214–1222.
47. Juvet SC, Moshkelgosha S, Sanderson S, Hester J, Wood KJ, Bushell A. Measurement of T cell alloreactivity using imaging flow cytometry. *J Vis Exp* 2017;122:55283.
48. Righi I, Vaira V, Morlacchi LC, Croci GA, Rossetti V, Blasi F, *et al.* Immune checkpoints expression in chronic lung allograft rejection. *Front Immunol* 2021;12:714132.
49. Mei YZ, Zhang XR, Jiang N, Cheng JP, Liu F, Zheng P, *et al.* The injury progression of T lymphocytes in a mouse model with subcutaneous injection of a high dose of sulfur mustard. *Mil Med Res* 2014;1:28.
50. Choy JC, Yi T, Rao DA, Tellides G, Fox-Talbot K, Baldwin WM III, *et al.* CXCL12 induction of inducible nitric oxide synthase in human CD8 T cells. *J Heart Lung Transplant* 2008;27:1333–1339.
51. Lillehoj EP, Kato K, Lu W, Kim KC. Cellular and molecular biology of airway mucins. *Int Rev Cell Mol Biol* 2013;303:139–202.
52. Rogers DF. Physiology of airway mucus secretion and pathophysiology of hypersecretion. *Respir Care* 2007;52:1134–1146. [Discussion, pp. 1146–1149.]
53. Thornton DJ, Sheehan JK. From mucins to mucus: toward a more coherent understanding of this essential barrier. *Proc Am Thorac Soc* 2004;1:54–61.
54. Wu M, Lai T, Jing D, Yang S, Wu Y, Li Z, *et al.* Epithelium-derived IL17A promotes cigarette smoke-induced inflammation and mucus hyperproduction. *Am J Respir Cell Mol Biol* 2021;65:581–592.
55. Weber WM, Kracko DA, Lehman MR, Irvin CM, Blair LF, White RK, *et al.* Inhalation exposure systems for the development of rodent models of sulfur mustard-induced pulmonary injury. *Toxicol Mech Methods* 2010; 20:14–24.
56. Cukic V. The changes of arterial blood gases in COPD during four-year period. *Med Arh* 2014;68:14–18.
57. Lama VN, Belperio JA, Christie JD, El-Chemaly S, Fishbein MC, Gelman AE, *et al.* Models of lung transplant research: a consensus statement from the National Heart, Lung, and Blood Institute workshop. *JCI Insight* 2017;2:e93121.